Functional characterization of a "plant-like" HYL1 homolog in the cnidarian *Nematostella vectensis* indicates a conserved involvement in microRNA biogenesis

Abhinandan Mani Tripathi[1], Arie Fridrich[1,2], Magda Lewandowska[1,2], Yehu Moran[1,3]

[1]Department of Ecology, Evolution and Behavior, Alexander Silberman Institute of Life Sciences, Faculty of Science, The Hebrew University of Jerusalem, Jerusalem 9190401, Israel

[2]These authors contributed equally to this work

[3]Corresponding author: yehu.moran@mail.huji.ac.il

Keywords

Nematostella vectensis, HYL1, microRNA, miRNA biogenesis, Cnidaria

ABSTRACT

While the biogenesis of microRNAs (miRNAs) in both animals and plants depends on Dicer, a conserved RNAse III enzyme, its helping partner proteins are considered distinct for each kingdom. Nevertheless, recent discovery of homologs of Hyponastic Leaves1 (HYL1), a "plant-specific" Dicer partner, in the metazoan phylum Cnidaria challenges the view that miRNAs evolved convergently in animals and plants. Here we show that the HYL1 homolog Hyl1-like a (Hyl1La) is crucial for proper development and miRNA biogenesis in the cnidarian model *Nematostella vectensis*. Inhibition of Hyl1La resulted in arresting of metamorphosis in *Nematostella* embryos. Moreover, most miRNAs are significantly downregulated in Hyl1La knockdown animals. These results support the participation of cnidarian HYL1 homologs in miRNA biogenesis and points towards the function of this pathway in cnidarian development. Further, it suggests that the last common ancestor of animals and plants carried a HYL1 homolog that took essential part in miRNA biogenesis.

INTRODUCTION

MicroRNAs (miRNAs) are 21-24 nucleotides long small RNAs that are known to be involved in post-transcriptional gene regulation and play important roles in both plant and animal development (Alvarez-Garcia and Miska, 2005; Bartel and Bartel, 2003; Voinnet, 2009). The miRNA is transcribed by RNA polymerase II into a long primary transcript, which is further processed into miRNA precursor and finally sliced into ~22 nucleotide miRNA/miRNA* duplex (Bartel, 2004, 2018; Voinnet, 2009). The processing of miRNA varies between plants and animals (Moran et al., 2013). In animals, the biogenesis of miRNAs is compartmentalized as the processing occurs in both nucleus and cytoplasm. Within the nucleus, the RNase type III Drosha and its partner Pasha (also called DGCR8) constitute a microprocessor complex (Kim et al., 2009). This complex acts on primary miRNA transcripts and process them into a precursor. The precursor is then transported by Exportin 5 into the cytoplasm where they get processed into the mature miRNA by the RNase type III Dicer with the help of other double-stranded RNA binding proteins such as Loquacious (Loqs), TRBP and PACT in the cytoplasm (Han et al., 2004a; Redfern et al., 2013; Saito et al., 2005). Contrastingly, in plants both primary and precursor transcripts are processed into mature miRNA by a single RNase type III, called DICER-LIKE1 (DCL1) assisted by its partner the double-stranded RNA binding motif (DSRM)-containing protein HYL1 within the nucleus (Han et al., 2004b; Voinnet, 2009). In both plants and animals, the miRNA duplex interacts with Argonaute proteins (AGOs) and forms the RNA-induced silencing complex (RISC) in the cytoplasm. The RISC complex commences miRNA guided cleavage and/or translational inhibition of complementary targets genes (Kim et al., 2009).

The metazoan lineages of Bilateria and its sister group Cnidaria separated more than 600 million years ago (MYA). While Bilateria include the vast majority of animals, Cnidaria include sea anemones, corals, hydroids and jellyfish. The phylogenetic position of cnidarians makes them an important comparative group for inferring animal evolution. In a previous study we identified different components of miRNA biogenesis machinery in Cnidaria and observed that most bilaterian components have cnidarian homologs. However, cnidarians lack homologs of classical bilaterian Dicer protein partners such as PACT, Loqs or TRBP (Moran et al., 2013). Interestingly two homologs of HYL1 called Hyl1-Like a (NveHyl1La) and Hyl1-Likeb (NveHyl1Lb) were identified in the sea anemone *Nematostella vectensis* (Moran et al., 2013). Apart from this it was also found that cnidarian miRNAs possess several interesting features that are common to their counterparts in plants: cnidarian miRNAs and their targets show perfect complementarity and frequently regulate their targets by mRNA cleavage (Moran et al., 2014). Recently, some other common features with plants that were identified in *Nematostella* included methylation of miRNAs by HEN1 (Modepalli et al., 2018), a feature rarely found in animals and the origin of miRNAs from inverted duplication of their target genes (Fridrich et al., 2020), a feature previously considered specific to plant miRNAs.

In addition to the presence of HYL1 homologs in Cnidaria, homologs are also present in other non-bilaterian animals such as sponges (*Amphimedon queenslandica*) and in ctenophores (*M. leidyi*) (Fig. 1; Ref. (Moran et al., 2013). However, we could not detect HYL1 homologs in Placozoa (*T. adhaerens*) (Figure 1a). Additionally, we also could not find any homologs in bilaterian animals and in unicellular organism like Fungi and Ichthyosporea. However, deep phylogenetic study of DSRM proteins showed that the protozoans and fungi are phylogenetically closer to the DSRM protein of plants (Dias et al., 2017). These results suggested that the HYL1-like proteins were already present in the common ancestor of plants and animals which during evolution has been lost in Bilateria and Ichthyosporea. These sequence-based observations led us to experimentally test the function of a HYL1 homolog of *Nematostella,* which could provide better insight into the evolution and origin of the miRNA biogenesis pathway.

RESULTS AND DISCUSSION

Hyl1La play an essential role in *Nematostella* development

Mutants of miRNA biogenesis pathway components exhibit severe developmental defects in both plants and animals (Alvarez-Garcia and Miska, 2005; Schauer et al., 2002). HYL1 protein has been known to play an essential role in growth and development of the model plant *Arabidopsis thaliana* by regulating miRNA biogenesis (Achkar et al., 2018; Han et al., 2004b). Similarly, in mice, TRBP mutants show

multiple developmental abnormities and reduction in miRNA accumulation (Koscianska et al., 2011; Zhong et al., 1999). The Hyl1La gene of *Nematostella* contains 11 exons and 10 introns translating into protein containing three DSRM domains (Figure 1b and Figure 2a). Unlike its paralog Hyl1Lb that is specific to stinging cells and carries unique protein domains, Hyl1La is ubiquitously distributed throughout *Nematostella* tissues and shares its domain structure with other cnidarian HYL1 homologs (Moran et al., 2013); therefore, we decided to focus our analysis on this gene. To decipher the function of Hyl1La in *Nematostella*, we designed two different splicing morpholino (Hyl1La SI MO1 and Hyl1La SI MO2) to knockdown by mis-splicing the gene at two different intron-exons junctions. Additionally, the gene was also targeted for inhibition by using the translation-blocking morpholino (Hyl1La TB MO) which binds on the 5′ UTR and sterically blocks the translation (Figure 2a). We injected each of the three MOs in *Nematostella* zygotes in parallel with a control morpholino (Control MO) designed to bind no target in the sea anemone genome. The effect of SI MOs was validated by PCR followed by cloning and sequencing which revealed in both cases intron retention (Figure S1 and Table S1). All the injected animals were studied until nine days post-fertilization (dpf). We observed that more than 80% of the animals injected with control MO developed normally and metamorphosed into primary polyps. In contrast, the animals injected with any of the three Hyl1La MOs showed developmental abnormalities where more than 90% of the animals did not develop into primary polyp until nine dpf (Figure 2b-e). The developmental abnormalities observed here were grossly similar to those observed in morphants of other miRNA processing components such as HEN1, Dicer1 and AGO knockdown animals (Fridrich et al., 2020; Modepalli et al., 2018). These results indicated that Hyl1La plays an essential role in *Nematostella* development, possibly by regulating the processing and expression of miRNAs.

Hyl1La regulates the miRNA biogenesis

The above observed developmental defects suggested the possible involvement of Hyl1La in miRNA biogenesis, as mutants defective in their miRNA biogenesis exhibit abnormal development in both animals and plants (Achkar et al., 2018; Zhong et al., 1999). The HYL1 in *Arabidopsis* interacts with the stem region of miRNA precursor by using its DSRM domains and woks with DCL1 synergistically (Song et al., 2007). Although the Dicer alone is capable of processing the precursor into mature miRNA, the presence of HYL1 enhances the accuracy as well as efficiency of miRNA biogenesis in plants (Dong et al., 2008). To assay the possible role of Hyl1La on miRNA expression in *Nematostella*, we performed small RNA sequencing of animals, injected with Hyl1La SI MO1 and with control MO. The analysis of read length distribution showed that the small RNA reads that lied between the size of miRNA (20-24nt) were higher ($P < 0.01$) in control as compared to knockdown embryos. Interestingly, the small RNAs that lie in the range of piRNAs (26-30nt) were slightly higher ($p = 0.0428$) in Hyl1La MO (Figure 3a), indicating

that knockdown of Hyl1La MO affects negatively the biogenesis of miRNAs but increases piRNA reads, as those small RNAs are produced by different machinery. We suggest this is probably due to more sequencing reads available for piRNAs following the decrease in miRNAs. Further, we analyzed the miRNA expression by using miRProf (Stocks et al., 2012) and normalized the miRNA reads in transcripts per million (TPM) (Table S2). For the miRNA quantification we used the most recent *Nematostella* miRNA datasets that were obtained by AGO-immunoprecipitation (Fridrich et al., 2020). The expression of normalized miRNA reads was compared between control and Hyl1La MO. About 54% of the total identified miRNAs showed downregulation of more than two-fold in Hyl1La MO injected animals as compared to the control (Figure 3b). A significant reduction in overall miRNA abundance was also observed in the knockdown mutants ($P < 0.00001$, Wilcoxon signed-rank test) (Figure 3c). The expression variation caused by the action of other two morpholinos (Hyl1La SI MO2 and Hyl1La TB) was also checked by quantitative stem-loop PCR of five miRNAs (Figure 3d and Figure S2). A significant downregulation of three miRNAs: miR2022-3p, miR2025-3p and miR2026-5p was found in all three MOs, which supported the small RNA sequencing results. In contrast, two miRNAs, miR2027-5p and miR2028-5p either showed upregulation or were not significantly affected by the Hyl1La knockdown. Previous studies have also shown that these two miRNAs respond similarly in HEN1 and Dicer knockdown morphants of *Nematostella* (Modepalli et al., 2018). The results of the present study, together with previous studies, establish the fact that these two miRNAs might be produced by some non-canonical miRNA biogenesis pathways. The presence of similar expression patterns for miRNA further strengthens our study and the involvement of Hyl1La in miRNA biogenesis. Further, we also checked for the processing accuracy of all the identified miRNA by mapping them onto their respective precursors. The analysis did not reveal aberrant processing. These results further suggested that like its homolog in plants, Hyl1La in *Nematostella* might be involved in enhancement of Dicer efficiency and is not involved in size selection.

To further support our results, we attempted to knockdown this gene by using short-hairpin RNAs (shRNAs), a method previously established in *Nematostella* (Karabulut et al., 2019). We designed three different shRNAs from three different regions of Hyl1La gene (Hyl1La shRNA1, Hyl1La shRNA2 and Hyl1La shRNA3) (Figure 4 a-c) and injected them into *Nematostella* zygotes. In parallel we also used a control shRNA with no target in *Nematostella* genome that was previously used as control for similar experiments (He et al., 2018; Karabulut et al., 2019). To assess the effect of these shRNAs on Hyl1La expression, we performed qRT-PCR from three days-old injected animals. Unexpectedly, we did not find any difference in Hyl1La expression (Figure 4d). Additionally, we also assessed the phenotype, but we could not identify any phenotypic difference as well. Next, we employed stem-loop PCR to test whether small RNAs are generated from an injected shRNA and indeed the small RNAs were produced as expected

(Figure 4e). Thus, the failure of the shRNAs to knockdown Hyl1La transcripts was probably not due to the lack of small RNA production from the shRNAs. The possible explanation of this contrasting result between MO and shRNA probably lies between the different mode of action of these two molecules. In contrast to MOs that do not use the cellular machinery, shRNA requires the miRNA/RNA interference machinery for their production as well as in target recognition and inhibition. Thus, our combined results suggest that Hyl1La might have an additional effect on biogenesis steps that are downstream to the cleavage by Dicer such as loading of small RNAs into AGO, the protein at the heart of the RNA-induced silencing complex (RISC) (Hutvagner and Simard, 2008). Under such a condition the shRNA derived small RNA would be unable to load onto RISC and hence could not cleave the Hyl1La, rendering its expression unaffected. Further, in such a scenario after injection with the shRNAs the system might reach a balance point that is very close to the normal Hyl1La levels. Alternatively, it is possible that the three shRNAs are ineffective due to lack of accessibility of the three distinct target sites on the Hyl1La transcript to the RISC loaded with the shRNA derived small RNAs for unknown reasons.

Altogether the absence of animal-like Dicer partner proteins such as TRBP or PACT and presence of a functional homolog of HYL1 (Hyl1La) in *Nematostella* indicated that a Hyl1-like protein might have been present in the last common ancestor of plants and animals. Apart from *Nematostella*, the presence of HYL1 homologs in additional members of Cnidaria and other non-bilaterian metazoan groups such as sponges (Figure 1a) further strengthens the notion of common ancestry of the miRNA systems of plants and animals. Further, unlike the cleavage mode of action and nearly-perfect target binding that could have evolved convergently in plants and cnidarians (Moran et al., 2014) due to functional constraints, the involvement in miRNA biogenesis of the Hyl1L in Cnidaria and its plant homolog HYL1 is far less likely to be the result of parallel evolution as it will require the independent recruitment of the same protein into the same system. Recently, it was found in *Chlamydomonas* (a unicellular green algae) that DUS16, which is a DSRM protein, and DCL3 were efficient enough for miRNA processing (Yamasaki et al., 2016). Further, various fungal groups also exhibit the presence of Dicer and plant-like DSRM proteins and lack animal-like accessory proteins, such as Drosha and Pasha (Dang et al., 2011; Dias et al., 2017). Contrastingly, DCL3 of *Chlamydomonas* exhibits some structural features that are reminiscent of metazoan Drosha (Valli et al., 2016). These observations suggest that the common ancestor of all these groups might have harbored only a single Dicer/Drosha-like RNAse III enzyme assisted by a DSRM protein resembling the ones found in plants (HYL1-like).

Finally, here we report that Hyl1La play an important role in miRNA biogenesis in *Nematostella*, a representative of Cnidaria which is the sister group of Bilateria. However, the functional importance of Hyl1La in *Nematostella* identified here raises another interesting evolutionary question of why Hyl1La was

replaced by other DSRM proteins like TRBP, Loqs or PACT in bilaterian animals during evolution (Figure 1a). Interestingly, both Loqs in flies and TRBP in mammals, enable processing of some miRNA precursors into different mature miRNAs and by this significantly increase their variability and targeted sequences (Fukunaga et al., 2012; Lee and Doudna, 2012). Such variability is currently unknown in plants or cnidarians. It is intriguing to consider the possibility that this ability of the bilaterian proteins to increase small RNA variability was advantageous over Hyl1-like proteins and led to the loss of the latter in bilaterian lineages.

SUPPLEMENTAL INFORMATION

Supplementary information includes two figures and three tables (Table S1, Table S2 and Table S3).

ACKNOWLEDGMENTS

The authors would like to thank Dr. Michal Bronstein and Ms. Adi Turjeman of the Center for Genomic Technologies (The Hebrew University) for their help with sequencing. The authors would also like to thank Dr. Reuven Aharoni (The Hebrew University) for his technical and administrative assistance in this work. This work was supported by European Research Council Starting Grant 637456 CNIDARIAMICRORNA to YM.

AUTHOR CONTRIBUTIONS

Conceptualization: A.M.T. and Y.M.; Methodology: A.M.T. and Y.M.; Validation: A.M.T.; Software: A.M.T. and A.F.; Formal Analysis: A.M.T., A.F. and M.L.; Investigation: A.M.T., A.F. and M.L.; Resources: Y.M.; Data Curation: A.M.T.; Writing –Original Draft: A.M.T. and Y.M.; Writing –Review & Editing: A.F. and M.L.; Visualization: A.M.T. and A.F.; Supervision: Y.M.; Project Administration: Y.M.; Funding Acquisition: Y.M.

DECLARATION OF INTERESTS

The Authors declare no competing interests.

REFERENCES

Achkar, N.P., Cho, S.K., Poulsen, C., Arce, A.L., Re, D.A., Giudicatti, A.J., Karayekov, E., Ryu, M.Y., Choi, S.W., and Harholt, J. (2018). A quick HYL1-dependent reactivation of microRNA production is required for a proper developmental response after extended periods of light deprivation. Developmental Cell *46*, 236-247. e236.

Alvarez-Garcia, I., and Miska, E.A. (2005). MicroRNA functions in animal development and human disease. Development *132*, 4653-4662.

Bartel, B., and Bartel, D.P. (2003). MicroRNAs: at the root of plant development? Plant Physiology *132*, 709-717.

Bartel, D.P. (2004). MicroRNAs: genomics, biogenesis, mechanism, and function. cell *116*, 281-297.

Bartel, D.P. (2018). Metazoan micrornas. Cell *173*, 20-51.

Chen, C., Ridzon, D.A., Broomer, A.J., Zhou, Z., Lee, D.H., Nguyen, J.T., Barbisin, M., Xu, N.L., Mahuvakar, V.R., and Andersen, M.R. (2005). Real-time quantification of microRNAs by stem–loop RT–PCR. Nucleic Acids Research *33*, e179-e179.

Dang, Y., Yang, Q., Xue, Z., and Liu, Y. (2011). RNA interference in fungi: pathways, functions, and applications. Eukaryotic Cell *10*, 1148-1155.

Dias, R., Manny, A., Kolaczkowski, O., and Kolaczkowski, B. (2017). Convergence of domain architecture, structure, and ligand affinity in animal and plant RNA-binding proteins. Molecular Biology and Evolution *34*, 1429-1444.

Dong, Z., Han, M.-H., and Fedoroff, N. (2008). The RNA-binding proteins HYL1 and SE promote accurate in vitro processing of pri-miRNA by DCL1. Proceedings of the National Academy of Sciences USA *105*, 9970-9975.

Fridrich, A., Modepalli, V., Lewandowska, M., Aharoni, R., and Moran, Y. (2020). Unravelling the developmental and functional significance of an ancient Argonaute duplication. BioRxiv.

Friedländer, M.R., Mackowiak, S.D., Li, N., Chen, W., and Rajewsky, N. (2012). miRDeep2 accurately identifies known and hundreds of novel microRNA genes in seven animal clades. Nucleic Acids Research *40*, 37-52.

Fukunaga, R., Han, B.W., Hung, J.-H., Xu, J., Weng, Z., and Zamore, P.D. (2012). Dicer partner proteins tune the length of mature miRNAs in flies and mammals. Cell *151*, 533-546.

Genikhovich, G., and Technau, U. (2009). Induction of spawning in the starlet sea anemone Nematostella vectensis, in vitro fertilization of gametes, and dejellying of zygotes. Cold Spring Harbor Protocols *2009*, pdb. prot5281.

Han, J., Lee, Y., Yeom, K.-H., Kim, Y.-K., Jin, H., and Kim, V.N. (2004a). The Drosha-DGCR8 complex in primary microRNA processing. Genes & Development *18*, 3016-3027.

Han, M.-H., Goud, S., Song, L., and Fedoroff, N. (2004b). The Arabidopsis double-stranded RNA-binding protein HYL1 plays a role in microRNA-mediated gene regulation. Proceedings of the National Academy of Sciences USA *101*, 1093-1098.

He, S., Del Viso, F., Chen, C.-Y., Ikmi, A., Kroesen, A.E., and Gibson, M.C. (2018). An axial Hox code controls tissue segmentation and body patterning in Nematostella vectensis. Science *361*, 1377-1380.

Hutvagner, G., and Simard, M.J. (2008). Argonaute proteins: key players in RNA silencing. Nature Reviews Molecular Cell Biology *9*, 22-32.

Karabulut, A., He, S., Chen, C.-Y., McKinney, S.A., and Gibson, M.C. (2019). Electroporation of short hairpin RNAs for rapid and efficient gene knockdown in the starlet sea anemone, Nematostella vectensis. Developmental Biology *448*, 7-15.

Kim, V.N., Han, J., and Siomi, M.C. (2009). Biogenesis of small RNAs in animals. Nature Reviews Molecular Cell Biology *10*, 126-139.

Koscianska, E., Starega-Roslan, J., and Krzyzosiak, W.J. (2011). The role of Dicer protein partners in the processing of microRNA precursors. PloS One *6*.

Lee, H.Y., and Doudna, J.A. (2012). TRBP alters human precursor microRNA processing in vitro. Rna *18*.

Livak, K.J., and Schmittgen, T.D. (2001). Analysis of relative gene expression data using real-time quantitative PCR and the 2− ΔΔCT method. Methods *25*, 402-408.

Modepalli, V., Fridrich, A., Agron, M., and Moran, Y. (2018). The methyltransferase HEN1 is required in Nematostella vectensis for microRNA and piRNA stability as well as larval metamorphosis. PLoS Genetics *14*, e1007590.

Moran, Y., Fredman, D., Praher, D., Li, X.Z., Wee, L.M., Rentzsch, F., Zamore, P.D., Technau, U., and Seitz, H. (2014). Cnidarian microRNAs frequently regulate targets by cleavage. Genome Research *24*, 651-663.

Moran, Y., Praher, D., Fredman, D., and Technau, U. (2013). The evolution of microRNA pathway protein components in Cnidaria. Molecular Biology and Evolution *30*, 2541-2552.

Plotnikova, A., Kellner, M.J., Schon, M.A., Mosiolek, M., and Nodine, M.D. (2019). MicroRNA dynamics and functions during Arabidopsis embryogenesis. The Plant Cell *31*, 2929-2946.

Redfern, A.D., Colley, S.M., Beveridge, D.J., Ikeda, N., Epis, M.R., Li, X., Foulds, C.E., Stuart, L.M., Barker, A., and Russell, V.J. (2013). RNA-induced silencing complex (RISC) Proteins PACT, TRBP, and Dicer are SRA binding nuclear receptor coregulators. Proceedings of the National Academy of Sciences USA *110*, 6536-6541.

Saito, K., Ishizuka, A., Siomi, H., and Siomi, M.C. (2005). Processing of pre-microRNAs by the Dicer-1–Loquacious complex in Drosophila cells. PLoS Biology *3*.

Schauer, S.E., Jacobsen, S.E., Meinke, D.W., and Ray, A. (2002). DICER-LIKE1: blind men and elephants in Arabidopsis development. Trends in Plant Science *7*, 487-491.

Song, L., Han, M.-H., Lesicka, J., and Fedoroff, N. (2007). Arabidopsis primary microRNA processing proteins HYL1 and DCL1 define a nuclear body distinct from the Cajal body. Proceedings of the National Academy of Sciences USA *104*, 5437-5442.

Stocks, M.B., Moxon, S., Mapleson, D., Woolfenden, H.C., Mohorianu, I., Folkes, L., Schwach, F., Dalmay, T., and Moulton, V. (2012). The UEA sRNA workbench: a suite of tools for analysing and visualizing next generation sequencing microRNA and small RNA datasets. Bioinformatics *28*, 2059-2061.

Valli, A.A., Santos, B.A., Hnatova, S., Bassett, A.R., Molnar, A., Chung, B.Y., and Baulcombe, D.C. (2016). Most microRNAs in the single-cell alga Chlamydomonas reinhardtii are produced by Dicer-like 3-mediated cleavage of introns and untranslated regions of coding RNAs. Genome Research *26*, 519-529.

Varkonyi-Gasic, E., Wu, R., Wood, M., Walton, E.F., and Hellens, R.P. (2007). Protocol: a highly sensitive RT-PCR method for detection and quantification of microRNAs. Plant Methods *3*, 12.

Voinnet, O. (2009). Origin, biogenesis, and activity of plant microRNAs. Cell *136*, 669-687.

Yamasaki, T., Onishi, M., Kim, E.-J., Cerutti, H., and Ohama, T. (2016). RNA-binding protein DUS16 plays an essential role in primary miRNA processing in the unicellular alga Chlamydomonas reinhardtii. Proceedings of the National Academy of Sciences USA *113*, 10720-10725.

Zhong, J., Peters, A.H., Lee, K., and Braun, R.E. (1999). A double-stranded RNA binding protein required for activation of repressed messages in mammalian germ cells. Nature Genetics *22*, 171-174.

METHODS

KEY RESOURCES TABLE

REAGENT or RESOURCE	SOURCE	IDENTIFIER
Bacterial Strain		
Escherichia coli DH5α	New England Biolabs	NEB-C2987I
Chemicals		
Trizol	Thermo (Ambion)	15596026
Tryptone	Merck Millipore	61930505001730
Yeast extract purified for Microbiology	Merck Millipore	61931105001730
Agar-Agar purified for Microbiology	Merck Millipore	61939005001730
Ampicillin	ROTH	K029.1
Dextran Alexa Fluor 488	Thermo (Molecular Probes)	D22910
Red sea salt	Red sea	N/A
L-Cysteine	Merck Millipore	1028380100
Critical Commercial Assay		
SuperScript III Reverse Transcriptase	Thermo (Invitrogen)	18080044
Fast SYBR® Green Master Mix	Thermo (ABI)	AB-4385612
Q5® High-Fidelity DNA Polymerase	New England Biolabs	NEB-M0493S
IVT kit	EPICENTRE	ASF3507
IVT purification kit	Zymo	R1054
Gel purification kit	Macherey-Nagel	MAN-740609.50
CloneJet cloning kit	Thermo (Fermentas)	K1231

NextSeq 500/550 v2 Kits (75 cycles)	Illumina	FC-404-2005
NEBNext Multiplex Small RNA Library Prep Set for Illumina (1-12) - 24 rxns	New England Biolabs	NEB-E7300S
Deposited Data		
Small RNA sequencing data	This study	NCBI-SRA PRJNA630340
Experimental Models: Organisms		
Nematostella vectensis	Lab strain, Rhode River, MD	Lab strain
Softwares		
miRProf	doi:10.1093/bioinformatics/bts311	http://srna-workbench.cmp.uea.ac.uk/
miRDeep2	doi:10.1093/nar/gkr688 (2012)	github.com/rajewsky-lab/mirdeep2
shRNA design	doi.org/10.1016/j.ydbio.2019.01.005	www.invivogen.com/sirnawizard/index
Domain Search	pfam.xfam.org/search#tabview=t	N/A
Homologs search	blast.ncbi.nlm.nih.gov/Blast.cgi/Proteins	N/A
Oligonucleotides		
PCR Primers	Integrated DNA Technologies	Supplementary Table S3
DNA template of shRNA	Integrated DNA Technologies	In this paper
Morpholino	Gene Tools	In this paper

LEAD CONTACT AND MATERIALS AVAILABILITY

Further information and requests for resources and reagents should be directed to and will be fulfilled by the Lead Contact, Yehu Moran (yehu.moran@mail.huji.ac.il). These resources and reagents will be made available upon request.

EXPERIMENTAL MODEL AND SUBJECT DETAILS

Nematostella vectensis (a common lab strain originating from Rhode River, MD) were grown in lab in 16‰ artificial seawater under controlled conditions. The knockdown animals (morphants) were generated by using the three different morpholinos. For cloning of splicing product, we used the DH5α *E. coli* cells provided by New England Biolabs (USA).

METHOD DETAILS

Animal culture and microinjection

Nematostella were in grown in 16‰ sea water at 18°C in a dark culture room. The growing animals were fed with freshly hatched *Artemia salina* nauplii three times a week. Induction of spawning was performed as previously described (Genikhovich and Technau, 2009): the mature male and female animals were induced to produce eggs and sperms by placing them in an incubator for eight hours under constant blue light and heat (25°C). After induction, the tanks were further kept in 18°C (in the culture room) for two hours to allow the release of egg packages and sperm. Further, the egg packages were fertilized for 30 min by placing the packages inside the male tanks. The quality of egg packages was checked under the stereomicroscope and egg packages of round shape and homogenous size were processed further for dejellying using 4% of L-Cysteine in 16‰ sea water pH 7.2 (titrated with NaOH). The selected eggs packages were kept in the cysteine solution for 45 min on a table shaker. The eggs were washed using 16‰ sea water in petri plates. These clean eggs (zygotes) were further used for injection. For injection 1mM (1000ng) stock solutions of both morpholino and shRNA were prepared by dissolving them into nuclease free water. The toxicity of morpholinos as well as shRNA was optimized by injecting different concentrations into the animals along with the control injected animals. The toxicity of less than 30% was considered suitable for injection. The morpholinos used here were designed and synthesized by Gene Tools, LLC (USA).

Hyl1La TB MO (Translation Blocking)	GGCCGCCATTTCTTAGAGAAGTTCA
Hyl1La SI MO1 (Splicing inhibition)	AGAAACAGACTTGTACCTTTTTGTA
Hyl1La SI MO2 (Splicing inhibition)	CTTGTTGTAGTCTAAGCCTTACCAT
Control MO (Standard control MO)	CCTCTTACCTCAGTTACAATTTATA

We found that optimum concentration was 300 μM, 900 μM and 450 μM for the Hyl1La TB, Hyl1La SI MO1 and Hyl1La SI MO2, respectively. For all the three shRNAs, 600 ng/μl concertation was found to be suitable. Similar concentration of control morpholino was used for injection in parallel with Hyl1La morpholinos. In every shift we injected 600 zygotes (300 Control MO and 300 Hyl1La MO) by

mixing the injected material with dextran Alexa Fluor 488 which was used as a fluorescent tracer while injection was carried under magnification by a TS-100F fluorescent microscope (Nikon, Japan). The injected zygotes were kept at 22°C for further growth. The morphology of the animals was observed up to nine days after which the number of settled and unsettled animals were counted and documented under SMZ-18 fluorescent stereomicroscope (Nikon). For RNA extraction injected zygotes were flash frozen in liquid nitrogen after three days of growth and stored at -80°C until RNA extraction. All the above experiments were performed in three independent biological replicates with three distinct animals' batches.

Small-RNA sequencing and analysis

The RNA was isolated using Trizol (Thermo Fisher Scientific) from three days old animals. Small RNA sequencing was performed for only Hyl1La SI MO1 and control MO injected animals. The small RNA library was prepared using NEBNext Multiplex Small RNA Library Prep Illumina kit (New England Biolabs) with some modifications (Plotnikova et al., 2019). In brief, small RNA was isolated (18nt-30nt) from 1µg of total RNA using 15% urea-PAGE (Bio-Rad) followed by overnight precipitation using 0.3% NaCl. The size selected small RNA was further precipitated using ice-cold ethanol (2.5x volume) and 1µl of GlycoBlue (Thermo Fisher Scientific) by centrifugation. The pellet was dissolved in 7.5 µl nuclease free water and used further for adapter ligation. The ligated products were subjected to 14 cycles of PCR amplification using adapter specific primers. The PCR product was run on 2% agarose gel followed by staining with GelRed (Biotium, USA). The band size between 137nt–149nt was selected and purified using Gel Extraction Kit (Macherey-Nagel, Germany). The quality of purified product (sRNA-seq libraries) was checked by using TapeStation system (Agilent, USA). The libraries having quality in range of the size (137nt–149nt) were used for sequencing. One ng of each sample was run on NextSeq500 (Illumina) in single end mode.

The small RNA data was analysed using miRProf (Stocks et al., 2012) with the following parameters: two mismatches allowed, minimum abundance 1, allowed overhang and not grouping mature and star stand. For mapping onto the genome and miRNA precursor for identification of aberrant processing of small RNAs miRDeep2 (Friedländer et al., 2012) was used. The miRNA expression was normalized in TPM (transcripts per million) by using only the transcripts that mapped on the reference genome. For read length distribution and scattered plot we used the average of expression obtained from the three biological replicates.

Synthesis of shRNA

Potential shRNA precursors for Hyl1La gene were predicted using the shRNA prediction tools (https://www.invivogen.com/sirnawizard/index.php) (Karabulut et al., 2019). Three precursors from three different regions were further chosen manually having GC% of more than 35%. Further, we also added the sequence for T7 promotor and three different mismatches at nucleotide position 10, 13 and 16 to create the bulges in precursors (Figure 4a-c). All these modified precursors were reverse complemented and synthesized by Integrated DNA Technologies (USA). The templates and reverse primer were mixed (1:1) and denatured at 98 °C for 5 min and cooled to 24 °C. Further, this mixture was mixed with the components of in-vitro transcription kit (Epicentre, USA) and incubated for eight hours at room temperature. The in-vitro transcribed product was further purified using the cleaning kit (Zymo Research, USA). The quality and size of the precursor was checked on agarose gel and its concentration were measured using Qubit Normal Sensitivity RNA Kit (Thermo, USA). The concentration ranged from 1500 ng to 2000 ng/µl.

Reverse transcription-quantitative PCR

For the quantification of Hyl1La transcripts from shRNA injected animals and for checking the splicing inhibition (Hyl1La SI MO injected animals), cDNA was prepared from 500 ng of total RNA using iScript™ cDNA Synthesis Kit (Bio-Rad, USA). For the quantification of miRNAs and shRNA, we designed the stem loop primers for five different miRNAs and shRNA (Chen et al., 2005). For cDNA preparation, 100 ng of total RNA was reverse transcribed using the SuperScript™ III Reverse Transcriptase (Thermo Fisher Scientific). The specificity of the miRNA primers was determined by using end point PCR (Varkonyi-Gasic et al., 2007). For this, we used 2 µl of cDNA as template, miRNAs specific forward primer and stem-loop specific reverse primer and run the PCR at 94°C for 2 min, followed by 35 cycles of 94°C for 15 s and 60°C for 1 min. For analyzing differential expression, we ran qRT-PCR with 5sRNA as internal control. For all the real time experiments, we used Fast SYBR® Green Master Mix (Thermo Fisher Scientific) and samples were run on StepOnePlus Real-Time PCR System (Thermo Fisher Scientific). All the real time experiments were performed in three independent replicates and data was analyzed using $2^{-\Delta\Delta Ct}$ method (Livak and Schmittgen, 2001). All the primers are listed in Table S3.

Cloning and sequencing of Hyl1La SI MO injected animals

To validate the effect of splicing morpholinos, we designed the primers pairs spanning the introns lying on the boundary of exons. PCR of the Hyl1La was done using Q5® High-Fidelity DNA Polymerase (New England Biolabs, USA). The PCR products were run on the gel and the expected-sized PCR product was purified with kit. Then the purified PCR products were ligated into the pJet2.1 vector (Thermo Fisher Scientific) and transformed into the *E. coli* DH5α strain of and outsourced for Sanger sequencing (HyLabs, Israel).

QUANTIFICATION AND STATISTICAL ANALYSIS

For statistical analysis of qRT-PCR data, Student's t-test was performed on ΔCt values between different comparisons. For phenotypic analysis we performed Student's t-test between the number of developed and undeveloped animals. To check overall significant difference between the miRNA expression levels, Wilcoxon signed-rank test was done. The Student's t-test was conducted in excel while Wilcoxon signed-rank test was done using socscistatistics (https://www.socscistatistics.com/tests/signedranks/default.aspx).

DATA AND CODE AVAILABILITY

The small RNA sequencing data were submitted to NCBI-SRA under BioProject ID PRJNA630340.

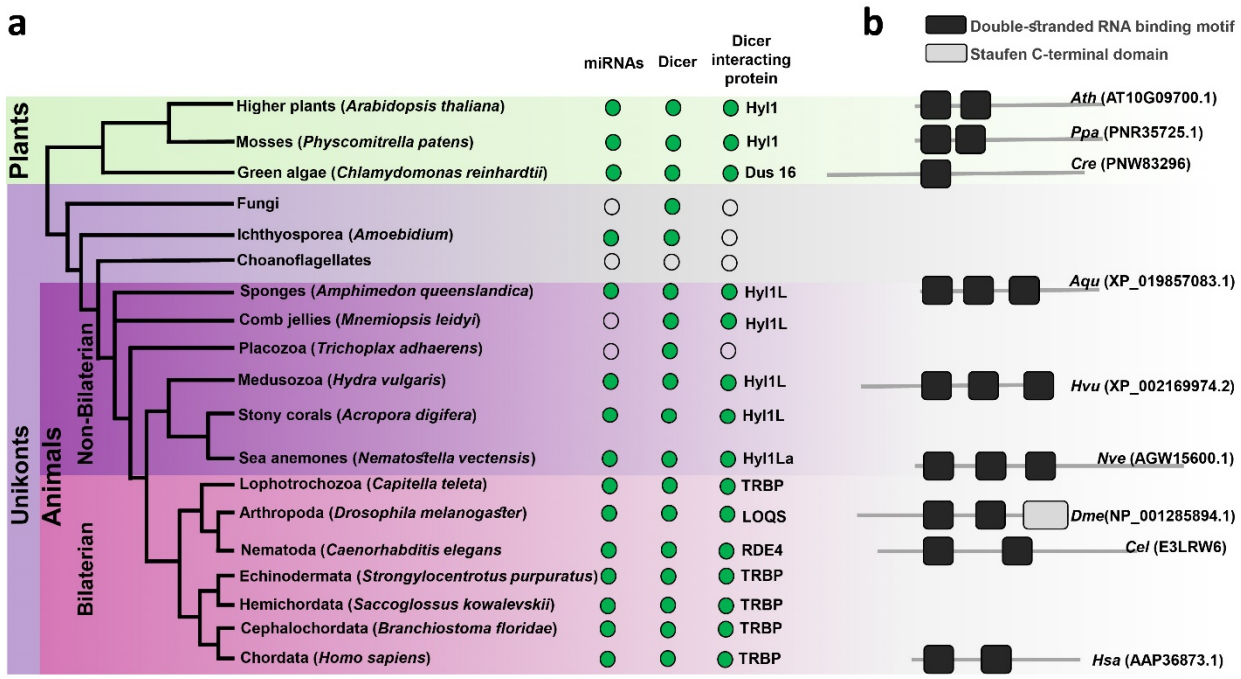

Figure 1. Schematic representation of phylogenetic tree of Eukaryotes at the phylum level

(a) Phylogenetic tree representing the presence (green circles) and absence (open circles) of miRNA, Dicer and Dicer interacting protein in different plant and animal phyla. The names of often-studied organisms in different phyla are given in brackets. The names of Dicer interacting proteins are given near the green circles.

(b) Domain structure of different Dicer interacting proteins predicted by using the Pfam (https://pfam.xfam.org/). NCBI gene ID is shown in brackets.

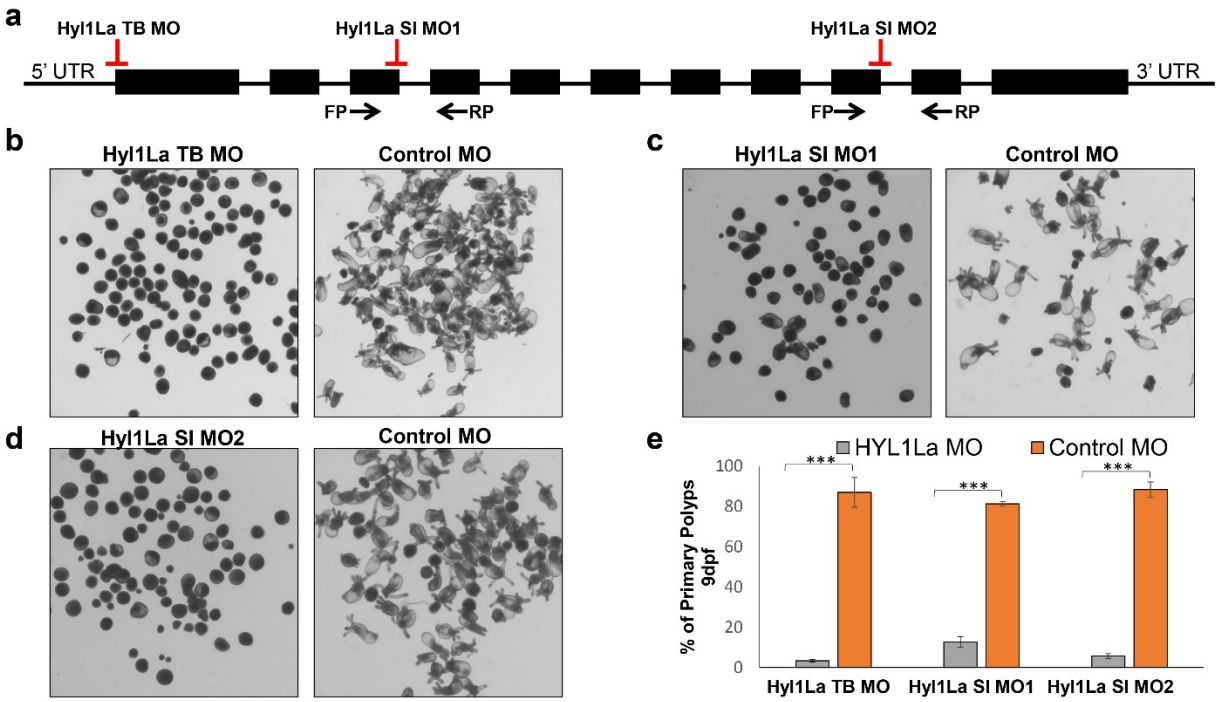

Figure 2. Developmental defects in different morphants of Hyl1La

(a) Schematic representation of the Hyl1La gene showing the intron-exon junction as defined by comparing the transcript (NCBI Accession KF192067.1) to the *Nematostella vectensis* genome. The positions targeted by different morpholinos used in the study are shown by red symbols. The black arrows represent the position of primers designed for the validation of splicing morpholino.

(b-d) Images of 9 dpf animals showing similar developmental defects in different morphants.

(e) Bar chart representing percentage of developed and undeveloped animals for each morphants. More than 80% of Hyl1La depleted animals did not develop into the primary polyp stage after 9 dpf. Data was taken in triplicates, in each n=200, ***P<0.001 (Student' t-test).

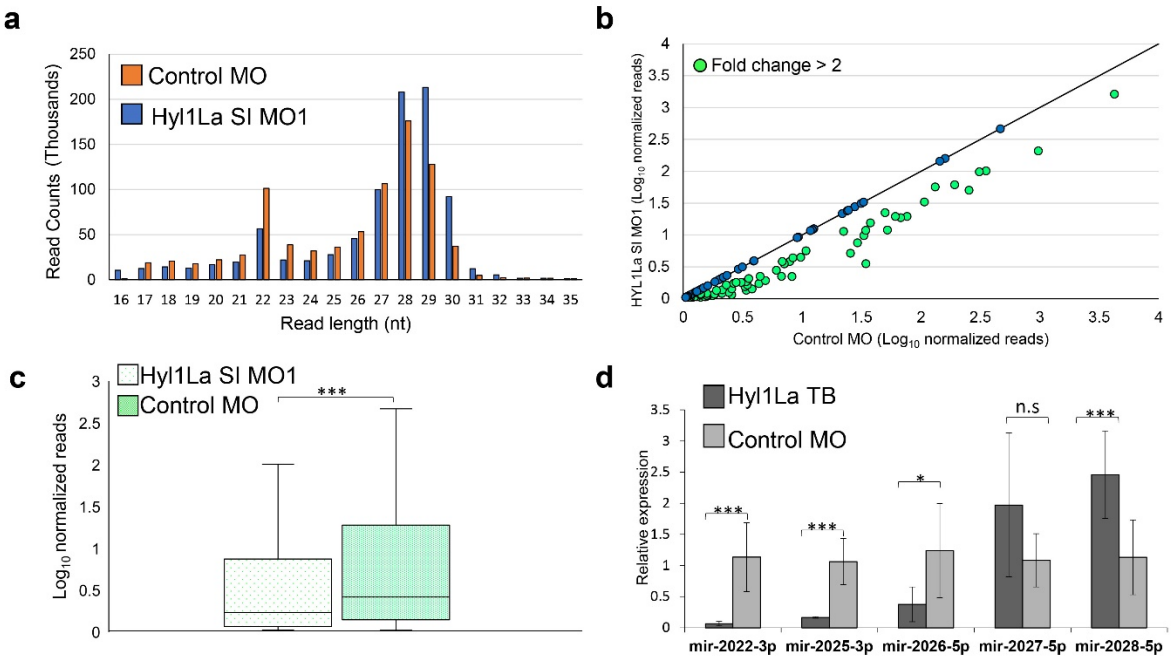

Figure 3. Hyl1La morphants show reduced expression of miRNA

(a) Average read length distribution of small RNA reads after adapter removal.

(b) Scatter plot representing normalized read counts of miRNAs in control and treated animals. Each dot represents the average expression of an individual miRNA. The miRNAs showing a depletion greater than two-fold are indicated in green. The axes are scaled to Log 10 of normalized read counts. The data represents the mean of three independent biological replicates.

(c) Box plot showing average of abundance of miRNA read counts in Hyl1La SI MO1 and control MO. A significant reduction of miRNA read counts is noted in Hyl1La SI MO1, ($P < .0001$, Wilcoxon signed-rank test). The data represents the mean of three independent biological replicates ± SD.

(d) Bar plot showing the expression of miR-2022, miR-2025, miR-2026, miR-2027 and miR-2028 as quantified using stem loop PCR in translation blocking (TB) and control morpholino. The data represents the mean of three independent biological replicates ± SD. ***$P<0.001$, ** $P \leq 0.01$. * $P \leq 0.05$, (Student's t-test), n.s (not significant).

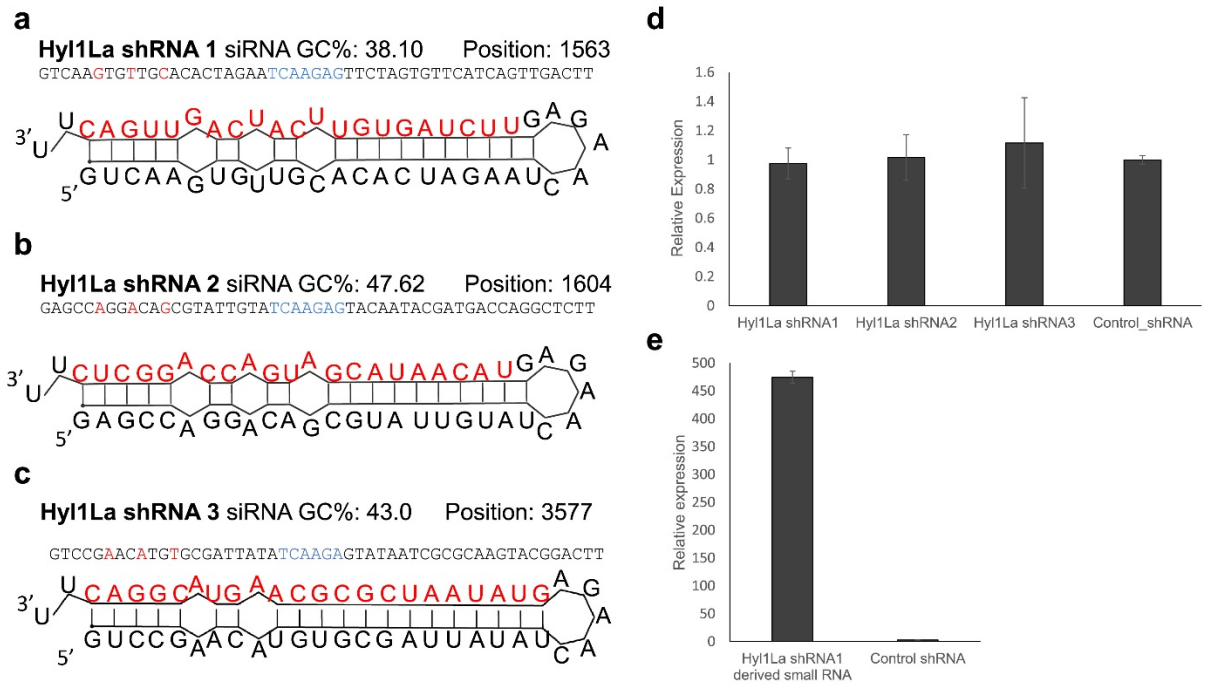

Figure 4. Structure of shRNA precursors and their effect on Hyl1La expression

(a-c) Structure of different shRNAs designed from different positions of Hyl1La gene along with GC content and their position are shown. In the shRNA sequence, the red colour shows the nucleotides edited for mismatch and blue colour represents loop region. The red coloured nucleotides on precursor's structure indicate the small RNA derived from the shRNAs.

(d) Real time quantification of Hyl1La from animals injected with different shRNAs relative to control. The data represents the mean of three independent biological replicates ± SD.

(e) Quantification of small RNA produced from Hyl1La shRNA1. The quantification was performed by using stem loop qRT-PCR.

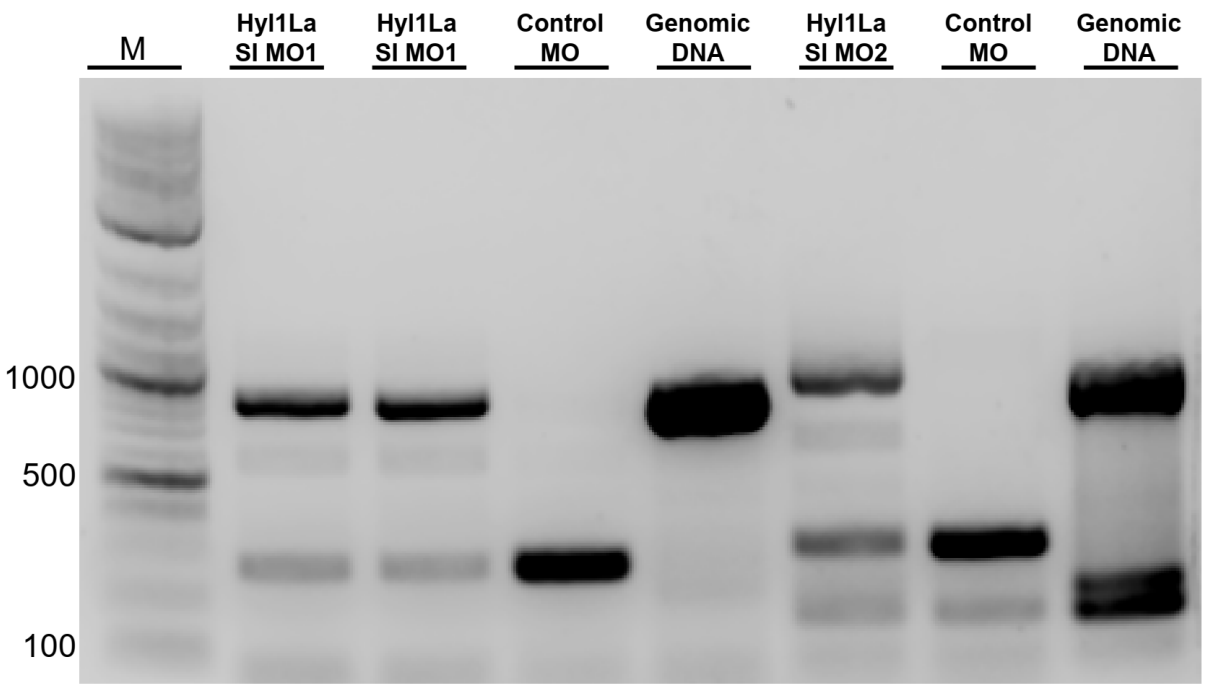

Figure S1. Gel image showing aberrant splicing of Hyl1La. Related to Figure 2.

cDNAs were amplified by using two different primer sets for different morpholinos (Hy1La SI MO1 and Hyl1La SI MO2). The control morpholino lane showed the band of spliced Hyl1La while the Hyl1La SI morpholino lane showed the band of size equivalent for intron retention. The genomic DNA was amplified by using the same primer pairs to check the size and primer efficiency.

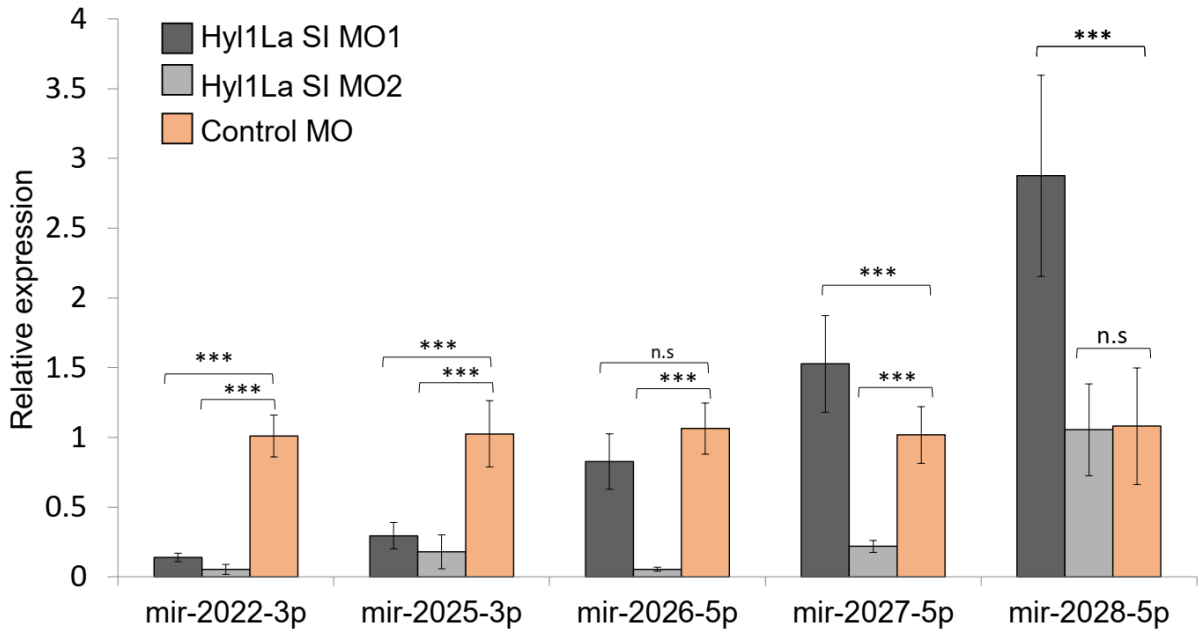

Figure S2. Effect of Hyl1La depletion on miRNA expression. Related to Figure 3.

The expression of miR-2022, miR-2025, miR-2026, miR-2027 and miR-2028 were checked by using the stem loop PCR between the Hyl1La SI MO1 vs. Control MO and Hyl1La SI MO2 vs. Control MO. The data represents the mean of four independent biological replicates ± SD. ***P<0.001, ** P ≤ 0.01. * P ≤ 0.05, (Student's t-test), n.s (not significant).